Nanoscale

COMMUNICATION

View Article Online
View Journal | View Issue

Check for updates

Cite this: *Nanoscale*, 2026, **18**, 5749

Received 31st October 2025,
Accepted 2nd February 2026

DOI: 10.1039/d5nr04609b

rsc.li/nanoscale

Open Access Article. Published on 17 Kudo 2026. Downloaded on 28/05/2026 5:22:09 AM.
This article is licensed under a Creative Commons Attribution 3.0 Unported Licence.

Synthesis and characterization of platinum-decorated iron carbide nanoparticles and their potential for magnetically induced catalysis

Sheng-Hsiang Lin, [a,b] Oscar Suárez-Riaño, †[c] Víctor Varela-Izquierdo, [c] Farzan Shabani,[c] Pier-Francesco Fazzini, [c] Edwin A. Baquero, [d] Simon Tricard, [c] Bruno Chaudret, *[c] Walter Leitner [a,b] and Alexis Bordet *[a]

A mild organometallic synthetic approach to platinum-decorated iron carbide nanoparticles (Pt@ICNPs) is reported. The resulting ferromagnetic Pt@ICNPs can be activated upon exposure to alternating current magnetic fields (ACMFs, magnetic induction), with a specific absorption rate of 625 W g^{-1} at 47 mT, 100 kHz. Pt@ICNPs are a versatile multifunctional platform with significant potential for applications in biomedicine and magnetically induced catalysis. The latter is demonstrated herein *via* the magnetically induced hydrogenation of various functionalities under mild conditions.

Platinum-containing nanoparticles (NPs) are important materials in electronic, energy storage, automotive, biomedicine, and chemical applications owing to their excellent electric, magnetic, and catalytic properties.[1] In particular, Pt NPs catalysts are pivotal to traditional automotive exhaust gases treatment,[2] petroleum refining,[3] electrocatalytic water splitting,[4] fuel cells,[5] and hydrogenation/dehydrogenation for liquid organic hydrogen carrier (LOHC) applications.[6] Pt is a rare and precious metal, prompting extensive efforts to improve the activity and durability of Pt NPs for more efficient catalytic utilization. A typical strategy is to immobilize Pt NPs on porous support materials to increase Pt dispersion and stability.[7–10] While relatively inert metal oxides and carbons have been widely used as support materials for catalytic NPs,[7,11] many opportunities arise once the support becomes functional,[12] and even stimuli-responsive.[13] In this context, core–shell NPs can combine multiple functions that do not exist in single-component compounds,[14] and there is growing interest in multifunctional NPs that respond to stimuli such as heat, light, electric, and magnetic fields, with the aim to enhance catalytic performance and decrease environmental impact.[15–18]

In particular, magnetically-responsive NPs coated or decorated with Pt are attractive in catalysis as they combine for instance efficient Pt utilization,[7] magnetic separation,[19] and potential magnetic heating capabilities upon exposure to alternating current magnetic fields (ACMFs).[18–20] In the past decades, various synthetic approaches have been reported for the preparation of Pt-decorated magnetic NPs (Pt@MagNPs), mainly using iron oxide NPs (IONPs) as the magnetic platform.[21] However, the moderate magnetic properties of IONPs lead to limited heat generation under magnetic induction, thereby limiting the potential of Pt@IONPs for magnetically induced catalysis. In addition, Pt deposition is typically achieved using high temperatures and non-sustainable reducing agents (*e.g.*, hydrazine and $NaBH_4$).[22–24] Thus, mild synthetic approaches to Pt@MagNPs with excellent magnetic properties are desirable, yet underdeveloped.

In this context, ferromagnetic iron carbide nanoparticles (ICNPs) possess the highest specific absorption rate (SAR) reported to date, and were showed to be excellent heating agents[25,26] and active species[27] in magnetically induced catalysis.[18,25–31] Organometallic synthetic routes were recently reported for the decoration of ICNPs with Ru or Cu to produce multifunctional Ru@ICNPs[30] and Cu@ICNPs[31] catalysts with great potential for magnetically induced hydrogenation and hydrodeoxygenation reactions.

Building on this approach, we explore herein the possibility to decorate ICNPs with Pt *via* a mild organometallic approach. The target Pt@ICNPs material must combine ICNPs' magnetic separation and heating capabilities with the excellent catalytic properties of Pt. This multifunctionality will be probed through the application of Pt@ICNPs to magnetically induced hydrogenation reactions of platform molecules under mild H_2 pressures (Fig. 1).

[a]*Max Planck Institute for Chemical Energy Conversion, Stiftstraße 34-36, 45470 Mülheim an der Ruhr, Germany. E-mail: alexis.bordet@cec.mpg.de*
[b]*Institute of Technical and Macromolecular Chemistry, RWTH Aachen University, 52074 Aachen, Germany*
[c]*Laboratoire de Physique et Chimie des Nano-Objets, Université de Toulouse, LPCNO, INSA, UPS, CNRS-UMR5215, 135 Avenue de Rangueil, 31077 Toulouse, France*
[d]*Estado Sólido y Catálisis Ambiental (ESCA), Departamento de Química, Facultad de Ciencias, Universidad Nacional de Colombia, Carrera 30 No. 45-03, 111321 Bogotá, Colombia*

† This work is dedicated to the memory of Oscar Suarez-Riaño, a scientist and friend whose passion and positive spirit greatly influenced our group.

Open Access Article. Published on 17 Kudo 2026. Downloaded on 28/05/2026 5:22:09 AM.
This article is licensed under a Creative Commons Attribution 3.0 Unported Licence.

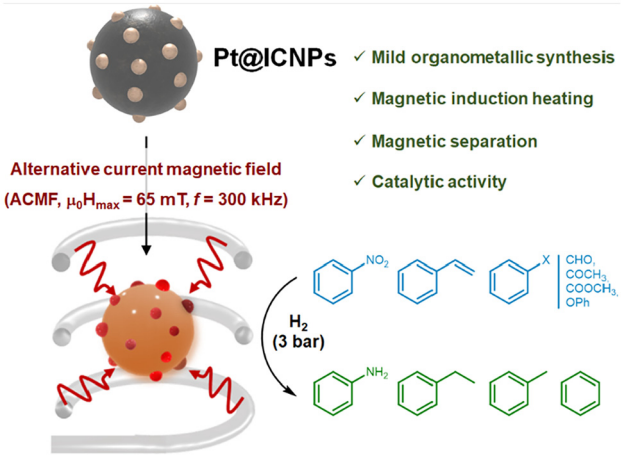

Fig. 1 Illustration of the approach followed in this study.

Pt-decorated ICNPs were synthesized through an organometallic approach (see SI Section S2). First, ICNPs ($Fe_{2.2}C@Fe_5C_2$ core@shell structure, *ca.* 15 nm) were prepared by carbidization of preformed Fe(0) NPs under syngas, following a reported procedure.[25] Then, a THF solution of *trans*-bis(benzonitrile)dichloroplatinum(II) (*trans*-$PtCl_2(NCPh)_2$), was added to a colloidal dispersion of ICNPs in THF, and the resulting mixture was pressurized with hydrogen (3 bar) at 30 °C for 16 h (Fig. 2). The organometallic precursor and reaction conditions were tuned to promote the controlled decomposition of the platinum complex at the ICNPs' surface, while suppressing side-nucleation of undesired free Pt NPs in solution (Fig. S1). Under suitable conditions (0.25 equivalent of Pt compared to Fe), homogeneous nucleation could be avoided, and Pt@ICNPs were obtained as a black magnetic powder (70% Fe, 4% Pt, and 26% ligands determined by scanning electron microscopy with energy-dispersive X-ray spectroscopy (SEM-EDX) and thermogravimetric analysis (TGA)).

Characterization of newly prepared Pt@ICNPs by transmission electron microscopy (TEM) showed small NPs (*ca.* 1.7 ± 0.3 nm) decorating the surface of larger core–shell structures typical of ICNPs (Fig. 2a). Scanning transmission electron microscopy in high-angle annular dark field mode (STEM-HAADF), along with elemental mapping by energy-dispersive X-ray spectroscopy (EDX), demonstrated the successful decoration of ICNPs with small Pt NPs (Fig. 2b–d). Powder X-ray diffraction (XRD) further evidenced the presence of both $Fe_{2.2}C$ and Pt(0) crystalline phases in the newly prepared material (Fig. 2e). X-ray photoelectron spectroscopy (XPS) analysis of the Fe 2p region of Pt@ICNPs showed the expected iron carbide peaks ($2p_{1/2}$ at 720.5 eV and $2p_{3/2}$ at 707.2 eV),[31,32] but also revealed the presence of $FeCl_x$ species (710.5 eV and 724.0 eV) presumably located at the nanoparticle surface (Fig. 2f and Fig. S2).[33] Analysis of the Pt 4f spectrum indicated platinum NPs in the metallic state (Fig. 2g),[34] consistent with the XRD data. Zero-field ^{57}Fe Mössbauer spectroscopy at 80 K showed the predominance of two iron carbide phases: $Fe_{2.2}C$ (68%) and Fe_5C_2 (25%), in the expected ratio for ICNPs,[25] along with minor contributions from paramagnetic iron species (5%, including the $FeCl_x$ species) and metallic iron

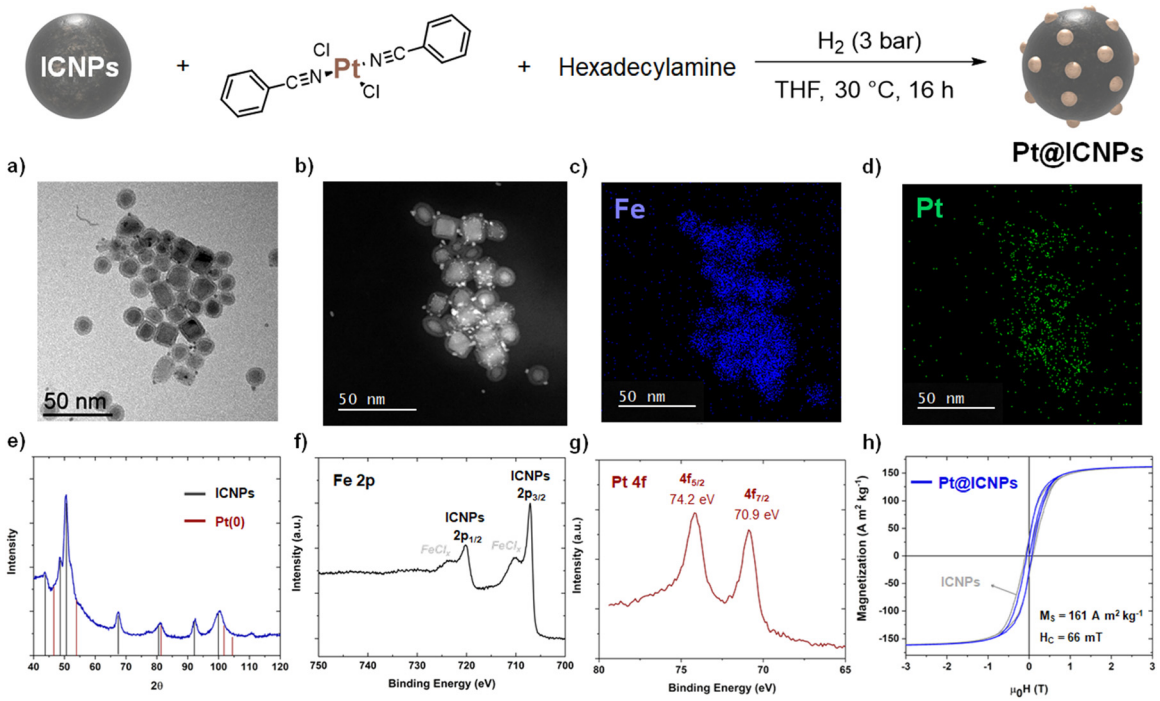

Fig. 2 Synthesis and characterization of Pt@ICNPs by (a) TEM, (b) STEM-HAADF, (c and d) STEM-HAADF images with EDX elemental mapping of (c) Fe Kα and (d) Pt Lα, (e) powder-XRD, (f) XPS of Fe (2p) region, (g) XPS spectra of Pt (4f) region and (h) Hysteresis curve at 300 K.

This journal is © The Royal Society of Chemistry 2026

Open Access Article. Published on 17 Kudo 2026. Downloaded on 28/05/2026 5:22:09 AM. This article is licensed under a Creative Commons Attribution 3.0 Unported Licence.

(2%) (Fig. S3). Signals corresponding to oxidized iron species were not detected, in agreement with XPS and XRD analysis. These data indicate that the morphology, composition, and structure of ICNPs did not change substantially upon Pt decoration.

Magnetic characterization by vibrating sample magnetometry (VSM) at 300 K showed that ICNPs decoration with Pt resulted in a slight reduction in the coercive field (H_C, from 94 mT to 66 mT) but no change in the saturation magnetization (M_S, 161 A m^2 kg$_{Fe}^{-1}$) (Fig. 2h and Table S1). While the surface $FeCl_x$ species may be responsible for the observed decrease in H_C,[35] the Pt@ICNPs are still ferromagnetic at room temperature. Furthermore, Pt@ICNPs demonstrated the ability to generate heat when exposed to ACMFs, with a SAR of 625 W g^{-1} measured at 47 mT and 100 kHz. This SAR value is lower than that of the starting ICNPs (>3000 W g^{-1}),[25] but remains higher than that of typical Fe_xO_y-based materials.[36] This includes Pt@IONPs (no heating, see SI) and Pt@Fe/FeO_x (109 W g^{-1}) prepared here as reference materials (see Section S2 for detailed synthetic protocols and Fig. S4 and S5 for characterization). This result is consistent with our previous reports where deposition of non-magnetic elements was shown to reduce the overall heating efficiency of the starting MagNPs.[30,31,37]

The potential of the newly prepared Pt@ICNPs for application in magnetically induced catalysis was explored through their testing in the hydrogenation of a variety of functional groups. Reactions were carried out in Fisher–Porter bottles under a standard set of reaction conditions: ACMF ($\mu_0 H_{max}$ = 65 mT, f = 300 Hz), 3 bar of H_2, 16 h, with decane as the solvent (Table 1). The global temperature of the reaction under the conditions mentioned, recorded with an infrared camera, was 200 °C; however, recent reports demonstrate that local hot spots could reach temperatures exceeding 300 °C.[27] Moreover, the magnetic nature of these Pt@ICNPs offers the possibility of easy recovery and separation from the reaction medium.

The C=C bond in styrene (**1**) and NO_2 group in nitrobenzene (**2**) were readily hydrogenated, giving the corresponding ethylbenzene (**1a**) and aniline (**2a**) products in quantitative yields.

Notably, Pt@ICNPs exhibited also hydrodeoxygenation (HDO) activity, enabling the selective reduction of aromatic compounds possessing aldehyde (benzaldehyde, **3**), ketone (acetophenone, **4**), and ester (methylbenzoate, **5**) functionalities to the corresponding methyl-substituted aromatic products. In the case of **3**, the selectivity toward toluene remained modest (31%), which is due to a competitive coupling reaction yielding 1,2-diphenylethane. This result demonstrates the formation of benzyl radicals during the deoxygenation process of benzaldehyde (Scheme S1).

The stability and reusability of Pt@ICNPs were investigated through recycling experiments using the HDO of **4** as a model reaction. While the catalyst was easily separated magnetically and reused through the cycles without any change in selectivity, severe loss of activity was observed after the 3rd cycle (Table S2). This loss of catalytic activity is attributed to the aggregation/coalescence and oxidation of Pt@ICNPs, as revealed by electron microscopy (Fig. S6), powder-XRD (Fig. S7), and VSM analysis (decrease of H_C (30 mT) and M_S (119 A m^2 kg$_{Fe}^{-1}$), Table S1 and Fig. S8). While the aggregation/coalescence of M@ICNPs is consistent with previous observations using other metals (*e.g.* Ru@ICNPs,[30] Cu@ICNPs,[31] *etc.*), NPs oxidation may have occurred due to handling during the recycling experiments/characterization.

Table 1 Hydro(deoxy)genation of various substrates using Pt@ICNPs activated by magnetic induction

#	Subs.	Prod.	Conv. (%)	Select. (%)
1	1	1a	>99	>99
2	2	2a	>99	>99
3	3	3a	>99	31[a]
4	4	4a	>99	>99
5	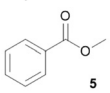 5	5a	>99	>99
6	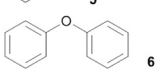 6	6a	23	>99
7	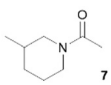 7	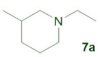 7a	0	0

Reaction conditions: Pt@ICNPs (10.0 mg, 0.002 mmol of Pt), substrate (0.33 mmol), decane (0.5 mL), 3 bar H_2, 65 mT, 300 kHz, 16 h. [a] Product distribution is provided in SI. Subs. = substrate. Prod. = product. Conv. = conversion. Select. = selectivity.

Notably, the selective HDO of **5** to toluene is interesting as it typically requires harsh reaction conditions under conventional heterogeneous catalysis,[38,39] while it is enabled under mild conditions by magnetically induced catalysis also with iron-based catalysts.[27] The magnetically induced hydrogenolysis of diphenylether (**6**) with Pt@ICNPs also proved possible, although challenging (23% conversion, >99% selectivity toward benzene). The excellent selectivity toward benzene indicates an efficient C_{sp^2}–OH bond cleavage and no aromatic hydrogenation activity, which is remarkable compared to previously reported catalytic and magnetocatalytic systems, which yielded complex mixtures of hydrogenated and non-hydrogenated products.[40–43] Notably, aromatic ring hydrogenation was suppressed in all the investigated cases, presumably due to a synergistic interaction between noble and 3d metals.[44,45] The hydrogenation of 1-acetyl-3-methylpiperidine (**7**) proved unsuccessful with Pt@ICNPs under these standard conditions, consistent with the difficulty of amide hydrogenation with H_2.[46,47] Notably, we have recently shown that the magnetically induced hydrogenation of amides can be enabled under mild conditions using a different catalyst design consisting in the immobilization of ICNPs as heating agents on a supported Pt catalyst.[48]

Open Access Article. Published on 17 Kudo 2026. Downloaded on 28/05/2026 5:22:09 AM. This article is licensed under a Creative Commons Attribution 3.0 Unported Licence.

Finally, reference Pt-decorated iron oxide nanoparticles (Pt@IONPs) prepared following an identical approach were found inactive for any reaction described here. The HDO of **4** could be catalysed by Pt@Fe/FeO_x (>99% ethylbenzene yield) but not the hydrogenolysis of **6** (Table S2). Pt@IONPs and Pt@Fe/FeO_x possess lower SAR than Pt@ICNPs, which results in insufficient thermal activation of the surface Pt for this challenging transformation. This comparison demonstrates the importance of selecting ICNPs with excellent magnetic properties to enable challenging transformation *via* magnetically induced catalysis.

Conclusions

In summary, we open a mild organometallic approach for the preparation of Pt-decorated iron carbide nanoparticles. Characterization of the novel Pt@ICNPs show that the morphology, composition, and structure of ICNPs do not change substantially upon Pt loading. Pt@ICNPs are ferromagnetic, and capable of heating efficiently upon exposure to ACMFs. Their potential for application in magnetically induced catalysis is demonstrated through the selective hydrogenation and hydrodeoxygenation of various functionalities under mild conditions. The importance of selecting ferromagnetic ICNPs as the magnetically-responsive core is outlined by the inactivity of reference Pt@IONPs under identical conditions. This work highlights the promise of magnetic NPs decoration as a versatile strategy for the design of novel multifunctional nanocatalysts.

Author contributions

S.-H. L. participated to the formulation of the original idea, project definition and conceptual planning of the experimental workflow, performed experimental work and data interpretation and wrote the manuscript draft. O. S. R., V. V-I., and F. S. performed experimental work and edited the manuscript. P.-F. F characterized the materials by electron microscopy. E. A. B., S. T., B. C., and W. L. participated to the data interpretation and editing of the manuscript. A. B. participated to the formulation of the original idea, project definition and conceptual planning of the experimental workflow, supervised the work, contributed to data interpretation and writing of the manuscript.

Conflicts of interest

There are no conflicts to declare.

Data availability

The data supporting this article have been included as part of the supplementary information (SI). Supplementary information is available. See DOI: https://doi.org/10.1039/d5nr04609b.

Acknowledgements

The authors acknowledge financial support by the Max Planck Society and by the Deutsche Forschungsgemeinschaft (DFG) under Germany's Excellence Strategy – Exzellenzcluster 2186 "The Fuel Science Center" ID: 390919832. A. B. acknowledges the Gordon and Betty Moore Foundation for financial support (GBMF ID #13905). Furthermore, the authors would like to thank Derya Demirbas (MPI-Kohlenforschung) for access and assistance with ^{57}Fe Mössbauer experiments, Dr. Lukas Pielsticker, Gudrun Klihm (MPI-CEC) for assistance with XPS experiments, Annika Gurowski, Alina Jakubowski, and Justus Werkmeister (MPI-CEC) for their support with GC and GC-MS measurements. S.-H. L. acknowledges NanoX for the mobility funding support. V. V. I. and B. C. are grateful to the French State aid managed by the Agence Nationale de la Recherche under France 2030 plan, bearing the reference code ANR-22-PESP-0010: Projet ciblé "POWERCO2" within the PEPR project SPLEEN. Open access funding enabled and organized by Projekt DEAL. Open Access funding provided by the Max Planck Society.

References

1 A. Chen and P. Holt-Hindle, *Chem. Rev.*, 2010, **110**, 3767–3804.
2 B. K. Cho, *Ind. Eng. Chem. Res.*, 1988, **27**, 30–36.
3 M. H. Pinzón, A. Centeno and S. A. Giraldo, *Appl. Catal., A*, 2006, **302**, 118–126.
4 K. L. Zhou, Z. Wang, C. B. Han, X. Ke, C. Wang, Y. Jin, Q. Zhang, J. Liu, H. Wang and H. Yan, *Nat. Commun.*, 2021, **12**, 3783.
5 T.-W. Song, C. Xu, Z.-T. Sheng, H.-K. Yan, L. Tong, J. Liu, W.-J. Zeng, L.-J. Zuo, P. Yin, M. Zuo, S.-Q. Chu, P. Chen and H.-W. Liang, *Nat. Commun.*, 2022, **13**, 6521.
6 Y. Wu, Y. Li, X. Yu, X. Ma, M. Boebinger, J. Webera and Z. Wu, *Catal. Sci. Technol.*, 2024, **14**, 1791–1801.
7 D. Leybo, U. J. Etim, M. Monai, S. R. Bare, Z. Zhong and C. Vogt, *Chem. Soc. Rev.*, 2024, **53**, 10450–10490.
8 L. Foppa, J. Dupont and C. W. Scheeren, *RSC Adv.*, 2014, **4**, 16583–16588.
9 X. Zhang, N. Hao, X. Dong, S. Chen, Z. Zhou, Y. Zhang and K. Wang, *RSC Adv.*, 2016, **6**, 69973–69976.
10 L. Liu, Y. Wang, Y. Zhao, Y. Wang, Z. Zhang, T. Wu, W. Qin, S. Liu, B. Jia, H. Wu, D. Zhang, X. Qu, M. Chhowalla and M. Qin, *Adv. Funct. Mater.*, 2022, **32**, 2112207.
11 H. Wang, Z. Gao, B. Sun, S. Mu, F. Dang, X. Guo, D. Ma and C. Shi, *Chem. Catal.*, 2023, **3**, 100768.
12 P. Verma, Y. Kuwahara, K. Mori, R. Raja and H. Yamashita, *Nanoscale*, 2020, **12**, 11333–11363.
13 P. Huang, R. Baldenhofer, R. P. Martinho, L. Lefferts and J. A. F. Albanese, *ACS Catal.*, 2023, **13**, 6590–6602.
14 Y. Zou, Z. Sun, Q. Wang, Y. Ju, N. Sun, Q. Yue, Y. Deng, S. Liu, S. Yang, Z. Wang, F. Li, Y. Hou, C. Deng, D. Ling and Y. Deng, *Chem. Rev.*, 2025, **125**, 972–1048.

 This journal is © The Royal Society of Chemistry 2026

Open Access Article. Published on 17 Kudo 2026. Downloaded on 28/05/2026 5:22:09 AM. This article is licensed under a Creative Commons Attribution 3.0 Unported Licence.

15 A. P. Blum, J. K. Kammeyer, A. M. Rush, C. E. Callmann, M. E. Hahn and N. C. Gianneschi, *J. Am. Chem. Soc.*, 2015, **137**, 2140–2154.
16 A. Bordet and W. Leitner, *Angew. Chem., Int. Ed.*, 2023, **62**, e202301956.
17 I. Salahshoori, A. Yazdanbakhsh, M. N. Jorabchi, F. Z. Kazemabadi, H. A. Khonakdar and A. H. Mohammadi, *Adv. Colloid Interface Sci.*, 2024, **333**, 103304.
18 A. Bordet, W. Leitner and B. Chaudret, *Angew. Chem., Int. Ed.*, 2025, **64**, e202424151.
19 L. Truong-Phuoc, C. Duong-Viet, J.-M. Nhut, A. Pappa, S. Zafeiratos and C. Pham-Huu, *ChemSusChem*, 2025, **18**, e202402335.
20 J.-S. Pavelić, S. Gyergyek, B. Likozar and M. Grilc, *Chem. Eng. J.*, 2025, **505**, 158928.
21 V. Polshettiwar, R. Luque, A. Fihri, H. Zhu, M. Bouhrara and J.-M. Basset, *Chem. Rev.*, 2011, **111**, 3036–3075.
22 R. Abu-Reziq, D. Wang, M. Post and H. Alper, *Adv. Synth. Catal.*, 2007, **349**, 2145–2150.
23 M. Xie, F. Zhang, Y. Longa and J. Ma, *RSC Adv.*, 2013, **3**, 10329–10334.
24 J. Adamski, M. I. Qadir, J. P. Serna, F. Bernardi, D. L. Baptista, B. R. Salles, M. A. Novak, G. Machado and J. Dupont, *J. Phys. Chem. C*, 2018, **122**, 4641–4650.
25 A. Bordet, L.-M. Lacroix, P.-F. Fazzini, J. Carrey, K. Soulantica and B. Chaudret, *Angew. Chem., Int. Ed.*, 2016, **55**, 15894.
26 H. Kreissl, J. Jin, S.-H. Lin, D. Schüette, S. Störtte, N. Levin, B. Chaudret, A. J. Vorholt, A. Bordet and W. Leitner, *Angew. Chem., Int. Ed.*, 2021, **60**, 26639.
27 S. Ahmedi, L.-M. Lacroix, D. Demirbas, D. J. SantaLucia, C. Weidenthaler, W. Hetaba, W. Leitner and A. Bordet, *J. Am. Chem. Soc.*, 2025, **147**, 34758–34766.
28 J. Mazarío, S. Ghosh, V. Varela-Izquierdo, L. M. Martínez-Prieto and B. Chaudret, *ChemCatChem*, 2025, **17**, e202400683.
29 C. Hu, Y. Dong, Q. Shi, R. Long and Y. Xiong, *Chem. Soc. Rev.*, 2025, **54**, 524–559.
30 J. M. Asensio, A. B. Miguel, P.-F. Fazzini, P. W. N. M. van Leeuwen and B. Chaudret, *Angew. Chem., Int. Ed.*, 2019, **58**, 11306.
31 S.-H. Lin, W. Hetaba, B. Chaudret, W. Leitner and A. Bordet, *Adv. Energy Mater.*, 2022, **12**, 2201783.
32 C. Yang, H. Zhao, Y. Hou and D. Ma, *J. Am. Chem. Soc.*, 2012, **134**, 15814–15821.
33 Y. J. Kim and C. R. Park, *Inorg. Chem.*, 2002, **41**, 6211–6216.
34 E. I. Vovk, A. V. Kalinkin, M. Yu. Smirnov, I. O. Klembovskii and V. I. Bukhtiyarov, *J. Phys. Chem. C*, 2017, **121**, 17297–17304.
35 T. Yanai, D. Fukushima, R. Narabayashi, N. Ogushi, Y. Yamaguchi, A. Yamashita, M. Nakano and H. Fukunaga, *AIP Adv.*, 2024, **14**, 025020.
36 R. Ghazi, T. K. Ibrahim, J. A. Nasir, S. Gai, G. Ali, I. Boukhris and Z. Rehman, *RSC Adv.*, 2025, **15**, 11587–11616.
37 V. Varela-Izquierdo, I. Mustieles-Marín, P.-F. Fazzini, G. Mencía, S. Guelen, R. Rachet and B. Chaudret, *Angew. Chem., Int. Ed.*, 2024, **63**, e202412421.
38 K. Sakoda, S. Yamaguchi, T. Mitsudome and T. Mizugaki, *JACS Au*, 2022, **2**, 665–672.
39 J. Pritchard, G. A. Filonenko, R. van Putten, E. J. M. Hensen and E. A. Pidko, *Chem. Soc. Rev.*, 2015, **44**, 3808–3833.
40 S. Ghosh, T. Ourlin, J. Mazarío, S. Cayez, S. Daccache, J. Carrey and B. Chaudret, *Chem. Mater.*, 2023, **18**, 7542–7553.
41 J. Mazarío, I. M. Marin, G. Mencia, C. W. Lopes, V. Varela-Izquierdo, G. Agostini, P.-F. Fazzini, N. Ratel-Ramond and B. Chaudret, *ACS Appl. Nano Mater.*, 2024, **8**, 9412–9427.
42 M. Guo, J. Peng, Q. Yang and C. Li, *ACS Catal.*, 2018, **8**, 11174–11183.
43 M. Wang, Y. Zhao, D. Mei, R. M. Bullock, O. Y. Gutiérrez, D. M. Camaioni and J. A. Lercher, *Angew. Chem., Int. Ed.*, 2020, **59**, 1445.
44 A. Bordet and W. Leitner, *Acc. Chem. Res.*, 2021, **54**, 2144–2157.
45 N. Marchenko, L.-M. Lacroix, N. Ratel-Ramond, W. Leitner, A. Bordet and S. Tricard, *ACS Appl. Nano Mater.*, 2023, **6**, 20231–20239.
46 M. C. Bryan, P. J. Dunn, D. Entwistle, F. Gallou, S. G. Koenig, J. D. Hayler, M. R. Hickey, S. Hughes, M. E. Kopach, G. Moine, P. Richardson, F. Roschangar, A. Steven and F. J. Weiberth, *Green Chem.*, 2018, **20**, 5082–5103.
47 J. R. Cabrero-Antonino, R. Adam, V. Papa and M. Beller, *Nat. Commun.*, 2020, **11**, 3893.
48 S.-H. Lin, S. Ahmedi, A. Kretschmer, C. Campalani, Y. Kayser, L. Kang, S. DeBeer, W. Leitner and A. Bordet, *Nat. Commun.*, 2025, **16**, 3464.